

Self-frequency blue-shift of dissipative solitons in silicon based waveguides

Samudra Roy¹, Andrea Marini¹ and Fabio Biancalana^{1,2}

¹Max Planck Institute for the Science of Light, Guenther-Scharowsky-Straße 1, 91058 Erlangen, Germany

²School of Engineering & Physical Sciences, Heriot-Watt University, EH14 4AS Edinburgh, United Kingdom

Compiled June 23, 2018

We analyze the dynamics of dissipative solitons in silicon on insulator waveguides embedded in a gain medium. The optical propagation is modeled through a cubic Ginzburg-Landau equation for the field envelope coupled with an ordinary differential equation accounting for the generation of free carriers owing to two-photon absorption. Our numerical simulations clearly indicate that dissipative solitons accelerate due to the carrier-induced index change and experience a considerable blue-shift, which is mainly hampered by the gain dispersion of the active material. Numerical results are fully explained by analytical predictions based on soliton perturbation theory. © 2018 Optical Society of America

OCIS codes: 190.5530, 190.4360, 130.4310, 230.4320

Silicon photonics has attracted considerable attention among researchers owing to its potential applications ranging from optical interconnection to bio-sensing. In the last few years, silicon-on-insulator (SOI) technology has rapidly developed into a well-established photonic platform [1]. The tight confinement of the optical mode and the inherently large bulk nonlinearity of Si tremendously enhance the nonlinear dynamics [2]. For near-infrared wavelengths in the range $1 \mu\text{m} < \lambda_0 < 2.2 \mu\text{m}$, two photon absorption (2PA) is the leading loss mechanism and limits the spectral broadening due to self-phase modulation (SPM) [3,4]. As a consequence of 2PA, electrons are excited to the conduction band, absorb light and affect the pulse dynamics by modifying the refractive index of silicon [5]. Loss mechanisms are restricted in silicon-organic hybrid slot waveguides, which can be exploited for all-optical high-speed signal processing [6]. Alternatively, loss can be overcome by embedding active materials in the design of SOI devices. Recently, some amplification schemes based on III-V semiconductors, rare-earth-ion-doped dielectric thin films and erbium-doped waveguides have been proposed and practically realized [7–9].

In this Letter, we describe for the first time to our knowledge the nonlinear dynamics of dissipative solitons (DSs) in amplifying SOI devices. DSs are stationary localized structures of open nonlinear systems far from equilibrium that can be observed in several contexts [10]. Although the model considered in our analysis is general and can be applied to any silicon-based amplifying setup, we specialize our calculations to a SOI waveguide embedded in Er-doped amorphous aluminium oxide ($\text{Al}_2\text{O}_3:\text{Er}^+$). Other gain schemes involving the use of semiconductor active materials can also be considered and gain dispersion can be reduced accordingly. For the representative structure displayed in Fig. 1, the gain bandwidth is of the order of 100 nm around the carrier wavelength $\lambda \simeq 1540$ nm. For this waveguide, the second order GVD coefficient and the effective area at $\lambda_0 = 1550$

nm are calculated to be $\beta_2 \simeq -2 \text{ ps}^2/\text{m}$, $A_{\text{eff}} \simeq 0.145 \mu\text{m}^2$, respectively. The proposed SOI waveguide is fabricated along the $[\bar{1}10]$ direction and on the $[110] \times [001]$ surface, so that quasi-TM modes do not experience stimulated Raman scattering (SRS) [5]. The propagation of an optical pulse with envelope $u(z, t)$ and carrier frequency ω_0 in the proposed photonic structure is governed by a complex Ginzburg-Landau (GL) equation,

$$i\partial_\xi u - \frac{1}{2}\text{sgn}(\beta_2)\partial_\tau^2 u + i\alpha u + (1 + iK)|u|^2 u + (i/2 - \mu)\phi_c u - i(g + g_2\partial_\tau^2)u = 0, \quad (1)$$

coupled with an ordinary differential equation accounting for the 2PA-induced free-carrier dynamics $d\phi_c/d\tau = \theta|u|^4 - \tau_c\phi_c$. Eq. (1) is written in dimensionless units, where the time (t) and the longitudinal spatial variable (z) are normalized to the initial pulse width ($t = t_0\tau$) and to the dispersion length ($z = \xi L_D$ with $L_D = t_0^2/|\beta_2(\omega_0)|$), respectively. The envelope amplitude (A) is rescaled to $A = u\sqrt{P_0}$, where $P_0 = |\beta_2(\omega_0)|/(t_0^2\gamma_R)$, $\gamma_R = k_0 n_2/A_{\text{eff}}$ with $n_2 \simeq (4 \pm 1.5) \times 10^{-18} \text{ m}^2/\text{W}$ is the Kerr nonlinear coefficient of bulk silicon. The bulk 2PA coefficient is $\beta_{\text{TPA}} \simeq 8 \times 10^{-12} \text{ m/W}$ and its corresponding effective waveguide counterpart $\gamma_I = \beta_{\text{TPA}}/(2A_{\text{eff}})$ is rescaled to the Kerr coefficient so that $K = \gamma_I/\gamma_R = \beta_{\text{TPA}}\lambda_0/(4\pi n_2)$. The linear loss coefficient (α_l) is renormalized to the dispersion length ($\alpha = \alpha_l L_D$) and can be neglected for short propagation in the linear transparency spectral window of silicon $1 \mu\text{m} < \lambda_0 < 10 \mu\text{m}$, where 2PA dominates (if $\lambda_0 < 2.2 \mu\text{m}$). The density of free-carriers (FCs) N_c generated through 2PA is normalized so that $\phi_c = \sigma N_c L_D$, where $\sigma \simeq 1.45 \times 10^{-21} \text{ m}^2$. FCs are responsible for free-carrier dispersion (FCD) regulated by the parameter $\theta = \beta_{\text{TPA}}|\beta_2|\sigma/(2\hbar\omega_0 A_{\text{eff}}^2 t_0 \gamma_R^2)$ [11] and free-carrier absorption (FCA) depending on the parameter $\mu = 2\pi k_c/(\sigma\lambda_0)$, where $k_c \simeq 1.35 \times 10^{-27} \text{ m}^3$ [12]. t_c is the characteristic FC recombination time (of the order of ns) and normalized as $\tau_c = t_0/t_c$, which we neglect in our calculations since we focus our analysis on ultrashort pulses with time duration of the order

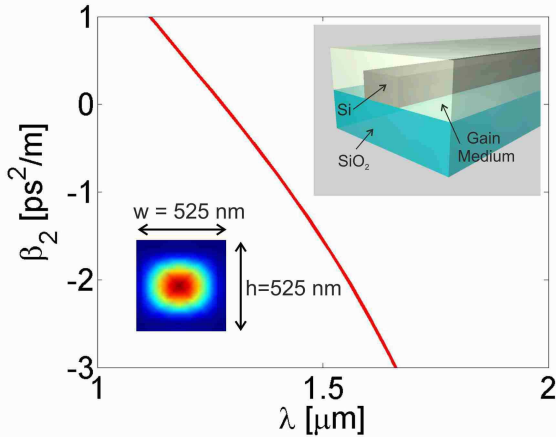


Fig. 1. Sketch of a SOI waveguide with lateral dimensions $h = w = 525$ nm surrounded by $\text{Al}_2\text{O}_3:\text{Er}^+$ and its dispersion property. The solid red line represents the group velocity dispersion (GVD) of the quasi-TM mode, whose spatial profile at $\lambda_0 = 1550$ nm is depicted in the inset below.

$t_0 \simeq 100$ fs. The amplifying medium is characterized by a gain coefficient G , which in our dimensionless equations is rescaled to the dispersion length ($g = GL_D$), and a dephasing time T_2 , which is related to the dimensionless gain dispersion coefficient through $g_2 = g(T_2/t_0)^2$.

The presence of gain and 2PA in the photonic structure considered in our calculations implies that, in general, energy is not conserved. The GL equation does not support solitons in a strict mathematical sense since it is not integrable by the inverse scattering transform. In contrast to Kerr solitons in conservative systems, which form continuous families of localized solutions, DSs are formed under a dynamical equilibrium involving non-trivial internal energy flows. DSs are associated with certain discrete parameters of the GL equation that satisfy the energy balance condition. In absence of linear loss (i.e. $\alpha = 0$) and free-carriers (i.e. $\phi_c = 0$), DSs can be found as $u(\xi, \tau) = u_0[\text{sech}(\eta\tau)]^{1-i\beta} e^{i\Gamma\xi}$, where the exact values of u_0, η, β, Γ are fixed by the physical parameters of the system g, g_2 and K [13]. This soliton suffers from inherent core and background instabilities and can be stabilized by introducing higher order nonlinearities or by coupling the system to a passive waveguide [14]. However, this task goes beyond the scope of the present work, where we aim at understanding the effect of FCs on the DS dynamics. In order to grasp the fundamental effects induced by FC dynamics, we develop a soliton perturbative analysis [15], approximating the GL equation as a perturbed nonlinear Schrödinger equation (NLSE): $i\partial_\xi u + \frac{1}{2}\partial_\tau^2 u + |u|^2 u = i\epsilon(u)$, where we explicitly consider the case of anomalous dispersion ($\beta_2 < 0$) and $\epsilon(u)$ includes the coupling to FCs, 2PA, linear gain and its dispersion: $\epsilon = (g - K|u|^2 - \phi_c/2 - i\mu\phi_c + g_2\partial_\tau^2)u$. The

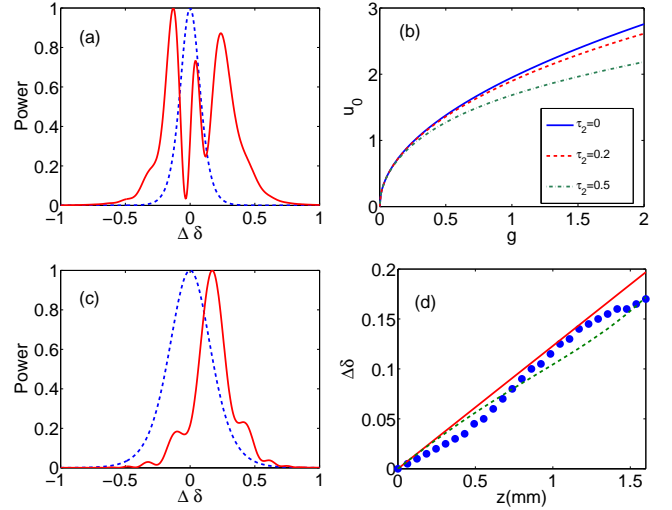


Fig. 2. (a) Asymmetric spectral broadening of the NLSE soliton ($u_{in} = \text{sech}\tau$) with time duration $t_0 = 40$ fs for $g = 1$ and $g_2 = 0$. (a) DS amplitude u_0 as a function of linear gain g for several dephasing times ($\tau_2 = T_2/t_0 = 0, 0.2, 0.5$) at fixed K . (c) Carrier-induced blue-shift of DS ($u_{in} = u_0[\text{sech}(\eta\tau)]^{1-i\beta}$) for the same parameters of (a), where $u_0 = \sqrt{3g/(2K)}$, $\eta = \sqrt{-g/\beta}$ and $\beta = 3/(2K) - \sqrt{[3/(2K)]^2 + 2}$. Solid red and blue dashed lines indicate the output and input power spectra, respectively. (d) z -dependent DS frequency shift ($\Delta\delta = \Omega/(2\pi)$) for $g_2 = 0$. Perturbative predictions with constant (solid red line) and z -dependent (green dotted line) peak amplitude u_0 are shown. The solid red dots indicate numerical findings.

perturbative theory is developed by making the *Ansatz*:

$$u(\xi, \tau) = u_0(\xi) [\text{sech} \{ \eta(\xi) [\tau - \tau_p(\xi)] \}]^{1-i\beta} \times e^{i\phi(\xi) - i\Omega(\xi)(\tau - \tau_p(\xi))}, \quad (2)$$

where the parameters $u_0, \eta, \tau_p, \phi, \Omega$ are now assumed to depend on ξ and $\epsilon(u)$ is considered as a small perturbation depending on u, u^* and their derivatives. The evolution dynamics of the soliton parameters over distance can then be predicted using the variational method [13], which leads to a set of coupled differential equations for the soliton parameters. The evolution of pulse energy (E), frequency (Ω) and temporal (τ_p) shifts are given by

$$\frac{dE}{d\xi} = -2E \left(\frac{1}{6}\theta u_0^2 E + g_2 \Omega^2 \right), \quad (3)$$

$$\frac{d\Omega}{d\xi} = \frac{8}{15}(\mu + \beta/2)\theta u_0^4 - \frac{4}{3}g_2(1 + \beta^2)\Omega\eta^2, \quad (4)$$

$$\frac{d\tau_p}{d\xi} = -(1 - 2g_2\beta)\Omega - \frac{7}{72}\theta E^2. \quad (5)$$

The perturbative analysis reveals that FCs induce frequency blue-shift and temporal acceleration of DSs, both effects being hampered by the gain dispersion that limits blue-shifting within the amplifying frequency window of the active material. For small gain dispersion, Eq. (4) is solved with the initial condition $\Omega(0) = 0$, obtaining $\Omega(\xi) = f\xi$, where $f = 8(\mu + \beta/2)\theta u_0^4/15$. This expression predicts that DSs experience a spec-

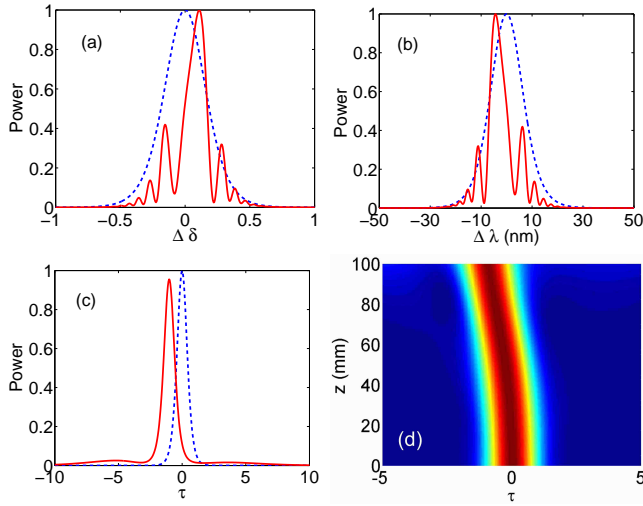


Fig. 3. (a,b) Input (dashed blue line) and output ($\xi = 5$, full red line) power spectrum of a dissipative soliton with carrier wavelength $\lambda_0 = 1550$ nm and time duration $t_0 = 200$ fs for $g = 1, g_2 = 0.04$ as a function of (a) dimensionless frequency and (b) physical wavelength. (c) Input (dashed blue line) and output ($\xi = 5$, full red line) temporal DS profile. (d) Intensity counterplot of the spatio-temporal evolution of an accelerated dissipative soliton.

tral blue-shift proportional to the propagation distance through a rate (f) that basically depends on the FC density. The equation of the temporal shift turns out to be $\tau_p(\xi) = -(a\xi + f\xi^2/2)$, where $a = 7\theta E^2/72$. The expression suggests during the propagation DS is accelerated under the influence of FCs analogously to the recently studied case of gas-filled hollow-core photonic crystal fibers [16].

In Fig 2a we show the conventional asymmetric spectral broadening of NLSE solitons [17]. In Fig. 2b we plot the DS amplitude (u_0) as a function of linear gain for several dephasing times ($\tau_2 = T_2/t_0 = 0, 0.2, 0.5$). As shown in Fig. 2c, even though DSs of the cubic GL equation are unstable, they experience a considerable carrier-induced blue-shift maintaining their shape over a propagation distance of the order of millimeters. Indeed, for DSs, 2PA is exactly compensated by the linear gain, while NLSE solitons experience an imbalanced dynamical evolution due to 2PA and amplification. In Fig. 2d we compare the perturbatively predicted FC-induced frequency blue-shift (full blue and dashed green lines) with numerical results (solid red dots), finding that for the initial part of pulse propagation, perturbative predictions nicely match with the numerical findings. The dimensionless frequency shift is calculated to be $\Delta\delta \simeq 0.16$ at $\xi = 2$, corresponding in physical units to $\Delta\lambda \simeq 35$ nm. The solid red line in Fig. 2d represents the predicted frequency shift calculated through the perturbation analysis by approximating the DS amplitude to remain constant, whereas the green dotted line represents the perturbative prediction considering z -dependent DS

amplitudes. From the very beginning of the propagation, the pulse shape is perturbed by FCD and FCA and hence the approximate analytic treatment fails for long propagation distances. Fig. 3 displays the effect of gain dispersion over the pulse propagation. Due to the finite bandwidth of the amplifying medium, the frequency shift is hampered after some saturation frequency (Ω_{sat}), as clearly predicted by our perturbative analysis: $\Omega(\xi) \simeq \Omega_{sat}(1 - e^{-\rho\xi})$, where $\Omega_{sat} = (\mu + \beta/2)\theta E^2/[10g_2(1 + \beta^2)]$ and $\rho = (4/3)g_2(1 + \beta^2)\eta^2$. In Figs. 3a,b we depict the input and output spectral power of a DS in presence of gain dispersion indicating that blue-shift is reduced, as predicted by the theory. In Fig. 3c we show the temporal profile of a propagating pulse at $\xi = 5$ where the inherent background instability of DSs starts to affect the pulse propagation. The spatio-temporal pulse evolution is displayed in Fig. 3d, where the pulse acceleration is reduced by the effect of gain dispersion.

In conclusion, we have provided a complete theoretical analysis of the the carrier-induced DS dynamics in Si-based waveguides embedded in an amplifying medium. FCs generated through 2PA affect the refractive index of the medium and lead to a considerable self-frequency blue-shift. We have derived analytical predictions for the self-frequency blue-shift and temporal evolution based on soliton perturbative theory. We also examined the fully realistic condition where gain dispersion hampers the continuous spectral blue-shifting, which is still observed.

This research was funded by the German Max Planck Society for the Advancement of Science (MPG).

References

1. B. Jalali, *J. Lightwave Technol.* **24**, 4600 (2006).
2. J. Leuthold, C. Koos and W. Freude, *Nat. Photon.* **4**, 535 (2010).
3. L. Yin and G. P. Agrawal, *Opt. Lett.* **32**, 2031 (2007).
4. C. Husko *et al.*, *Opt. Lett.* **36**, 2239 (2011).
5. Q. Lin, O. J. Painter and G.P. Agrawal, *Opt. Express* **15**, 16604 (2007).
6. C. Koos *et al.*, *Nat. Phot.* **3**, 216 (2009).
7. A. W. Fang *et al.*, *Mater. Today* **10**, 28 (2007).
8. K. Wörhoff *et al.*, *IEEE J. Quantum Electron.* **45**, 454 (2009).
9. L. Agazzi *et al.*, *Opt. Express* **18**, 27703 (2010).
10. N. Akhmediev and A. Ankiewicz, *Dissipative Soliton: Lecture notes in Physics*, (Springer, Birlin, 2005)
11. Q. Lin *et al.*, *Appl. Phys. Lett.* **91**, 021111 (2007).
12. M. Dinu *et al.*, *Appl. Phys. Lett.* **82**, 2954 (2003).
13. G. P. Agrawal, *Application of Nonlinear Fiber Optics*, 2nd ed. (Academic Press, San Diego, 2008).
14. B. A. Malomed and H. G Winful, *Phys. Rev. E* **53**, 5365 (1996).
15. H. Hasegawa and Y. Kodama, *Soliton in optical communication*, (Oxford University Press, New York, 1995).
16. M. F. Saleh *et al.*, *Phys. Rev. Lett.* **107** (2011).
17. C.A. Husko *et al.*, *Scientific Reports.* **3**, 1100 (2013).